Comparing the operation of aerobic granular sludge under different hydrodynamic regimes during the treatment of textile wastewater containing engineered silver nanoparticles

Miguel Alexandre Salvador Coelho | miguel.a.salvador.c@tecnico.ulisboa.pt

iBB – Institute for Bioengineering and Biosciences, Department of Bioengineering, Instituto Superior Técnico, Universidade de Lisboa, Av. Rovisco Pais, 1049-001 Lisbon, Portugal

Two aerobic granular sludge (AGS) sequencing batch reactors (SBRs) were operated for 192 days in order to investigate the effects of hydrodynamic regime (tested along the dimensions of hydrodynamic shear and anaerobic feeding strategy) and silver nanoparticle (Ag NP) loading over AGS properties and stability. SBRs were fed with a synthetic textile wastewater containing 10 mg Ag NPs L^{-1} under either a fast, static filling (SBR1) or a plug-flow filling configuration (SBR2); shear differences between the two systems were determined by stirring speeds (70 rpm in SBR1 and 280 rpm in SBR2). Granulation was achieved successfully in both SBRs without any impact from Ag NP addition. Lower shear stresses in SBR1 resulted in increased settleability, granulation and sludge N-acyl-L-homoserine concentrations over the first 50 days but proved irrelevant in driving sludge properties thereafter. Damaging effects over settleability – possibly caused by prolonged Ag NP dosing – were observed in the long term and caused severe washout episodes in both SBRs on day 85. This event initiated a period of cyclical sludge accumulation and washout which was likely driven by nanoparticle build-up and removal and which could point to a negative, concentration-dependent effect of Ag NPs over AGS stability. Finally, the plug-flow filling arrangement imposed on SBR2 was found to have a positive long-term effect on sludge density that reflected in superior sludge settleability.

Introduction

Textile wastewaters (TWWs) are characterized by high organic loads, high concentrations of recalcitrant dyes – mainly azo dyes – and a generally diverse chemical content. They represent one of the biggest contributions for water pollution worldwide and are currently the subject of intense research striving to develop suitable remediation strategies [1]. Among the available alternatives, the use of anaerobic-aerobic sequencing batch reactors (SBRs) for the bacterial decolorization of azo dye-laden TWWs is one of the most investigated. The process comprises two stages: the anaerobic cleavage of the dyes' azo bonds, resulting in the formation of colourless and often toxic aromatic amines, and the aerobic degradation of these metabolites [2]. Although the method has been known to provide consistently positive outcomes in what regards colour removal, aerobic aromatic amine conversion is a remarkably difficult process requiring the presence of specialized microbial strains and is often not achieved in process units [2]. Arylamines might therefore accumulate in wastewater treatment reactors to unleash their toxic action over the process biomass and can eventually find their way into receiving water bodies to interact with natural biota.

In addition to dye- and aromatic amine-related toxicity, the increasing occurrence of engineered nanoparticles in TWWs has been noted in recent years, sparking concerns for further negative impacts during and after treatment. A key example is that of silver nanoparticles (Ag NPs), a finishing additive used in a range of textile products that has been shown to penetrate and/or change the permeability of microbial cell membranes and to unleash a range of unspecific toxic effects through the release of Ag^{+} ions [3]. In the face of these concerns, aerobic granular sludge (AGS) SBRs, lauded for their ability to endure higher toxic loads than conventional activated sludge (CAS), have emerged as a promising solution for TWW treatment [1]. AGS systems can be developed from CAS inocula in response to an adequate balance of selective pressures, cell-to-cell interactions, and hydrodynamic shear forces and are normally established by manipulating a number of key operational conditions such as settling times, hydrodynamic shear stresses and periodic aerobic starvation conditions. The process of aerobic granulation results in the establishment of large, strong-structured biomass aggregates with regular outlines called aerobic granules (AGs), which are composed by densely packed, self-immobilized microbial consortia enmeshed in a net of extracellular polymeric substances (EPS) [4,5]. Owing to their unique structural properties, AGS systems are characterized by (*i*) an excellent settling behaviour, resulting in good solid–liquid separation over a short settling period and (*ii*) a good biomass retention capacity, allowing high accumulation in the SBR [1,4]. AGs are additionally characterized by independent aerobic and anoxic/anaerobic internal zones – developed as a result of oxygen mass transfer gradients along the EPS matrix – that provide unique conditions for the proliferation of multiple bacterial species with a capacity to degrade a wide range xenobiotic compounds, organics and nutrients [1,5,6]. These properties substantiate a strong incentive for the use of AGs in the bioremediation of aggressive industrial wastewaters. Promising results in the field of TWW treatment have been reported in recent years by several authors, highlighting increased opportunities for reductive decolourization in the deep, anaerobic reaches of AGs [7], the stabilizing action of azo dye substrates over the granular architecture [8] and, rather importantly, the establishment of aromatic amine-degrading bacterial populations over long operational periods (stemming from the increased sludge retention ability of AGS reactors) [1,8]. However, many questions regarding the workings of AG development and stability in general and during the treatment of Ag NP-laden TWWs specifically remain unanswered. Some of these questions can be summarized as follows.

The role of quorum sensing signalling in the formation and maintenance of AGs

Recent strides in AGS research have yielded important information regarding AG integrity and stability at the level of cell-to-cell

communication [9]. In one example, the concentration of AHLs, a common autoinducer produced by Gram-negative bacteria, was shown to increase with granulation [10] and AGS was demonstrated to have a higher content of AHLs than floccular sludge [11,12]. When an SBR was inoculated with floccular sludge and operated to promote AG development, strong positive correlations between EPS production and AHL concentrations were seen to arise over the course of granulation; likewise, over 50% of the 50 most common microbial isolates were shown to bear strong simultaneous positive correlations with at least one AHL and with granulation, pointing at a community level coordination of QS-regulated AG development [13]. Despite the wealth of information on granule formation, however, data on the relation between AG maintenance and decay and QS mechanisms is much sparser. In one of the most relevant examples out of the few, Tan *et al.* (2014) found AHL levels tended to drop during later stages of granule maturation and disintegration and once again observed a community shift during structural breakdown, favoring microorganisms that correlated negatively with granulation [13]. Likewise, very few studies have been published establishing the link between macroscopic operational conditions known to impact granule formation/stability and communicational responses at the microscopic level. In a rare example, AI-2 levels in AGs were shown to increase throughout the aerobic starvation stages of SBR cycles and to promote the production of EPS with high molecular weights, leading to cell adhesiveness enhancement and granule formation [14]. To patch some of these information holes, this work describes the analysis of sludge QS signal levels (specifically, AHL levels) over the course of a long-term operation in two SBRs operated according to different anaerobic feeding strategies (known, as discussed ahead, to impact on AG stability) and different hydrodynamic shear stresses (known, as previously stated, to impact AG development). The experimental design will include the identification of specific AHL production patterns associated with each of these conditions, both in an initial granulation phase and in the long run, and will be combined with other analytical methods to fully characterize sludge properties.

The impact of anaerobic feeding strategy over AG stability

Among the challenges currently facing the dissemination of AGS systems as the default treatment solution for industrial wastewaters, the development of structurally stable aerobic granules able to withstand long operation periods without losing their integrity or faltering in terms of treatment performance remains one of the toughest hurdles to clear [9,15]. The development of AGs with low microbial growth rates has been described as an effective strategy to ensure granule stability [16] and is nowadays regarded as a basic requirement in the field of AGS research [17]. The imposition of an anaerobic plug-flow filling stage followed by a prolonged aerobic reaction has been associated with improved structural stability in tubular SBRs (*i.e.*, SBRs with high height-to-diameter ratios) and linked to the selection of slow-growing heterotrophic microorganisms able to convert easily biodegradable substrates to slowly biodegradable storage polymers under anaerobic conditions (such as polyphosphate- and glycogen-accumulating organisms) [16]. However, recent studies have demonstrated that using this strategy in non-tubular reactors can actually be detrimental for sludge stability, leading to poor fluid distribution across the sludge bed and hindering anaerobic substrate consumption by target bacterial populations [18]. To avert this scenario, Rocktäschel *et al.* (2013) suggested the use of a stirred anaerobic stage immediately after filling in non-tubular bioreactors so as to secure a better substrate distribution across the working volume and ensure better anaerobic consumption by slow growers. The arrangement proved superior to anaerobic plug-flow filling alone, allowing for stable operation over a long period of time and suggesting the burden of substrate uptake can be transferred in large part from filling to the anaerobic reaction stage [18].

The contribution of the filling stage should, however, not be ignored when considering stability matters. In a recent study, Franca *et al.* (2017) compared the responses to perturbations in substrate composition and loading in two non-tubular SBRs set up with an anaerobic mixing period and fed according to one of two strategies – an anaerobic plug-flow or an anaerobic, fast and static filling arrangement. Plug-flow filling was shown to allow for faster AGS recovery in response to the imposed disturbances, with milder rebounds in terms of biomass concentration, sludge settling properties and sludge retention time than recorded in the latter bioreactor [19]. These results hint at a better case for long-term AG maintenance in association with a combined plug-flow filling/anaerobic mixing arrangement and substantiates a new and largely unexplored avenue for granule stabilization through anaerobic feeding. In an effort to advance the knowledge on this strategy, the present study was framed as a test to the reproducibility of the results described by Franca *et al.* (2017) [19] and as a deeper investigation of the drivers of granule stabilization specific to this strategy. The bioreactors employed in the original report were once again operated using a synthetic TWW – prepared with a hydrolysed, starch-based sizing agent, an azo dye and a high dose of Ag NPs – and fed with a nominally constant composition for 192 days to assess long-term process stability and eliminate the variability produced by changes in the feed solution. Stability was evaluated in terms of granule number and structure, macroscopic biomass properties (settleability and inventory) and treatment performance (as judged by COD and colour removal yields) and interpreted simultaneously as a product of feeding configuration and Ag NP loading. Context for the action of Ag NPs over granule stability will be provided in the following section.

The interaction and effects of Ag NPs over AGS

The interactions of Ag NPs with biological wastewater treatment systems have been investigated with ever more recurrence in recent years owing to their increased prevalence in both industrial and municipal effluents. Reported exposure effects run the gamut from unremarkable variations in sludge properties to significant shifts in microbial composition and pollutant removal depending on a number of factors such as nanoparticle physicochemical properties (*e.g.*, surface coatings, shape) and dosage [20]. Some consistent conclusions have, however, been reached. Microbes in attached-growth wastewater treatment systems appear, for instance, to be less susceptible to Ag NPs than suspended flocculent cultures. The physical structure of microbial aggregates – brought about by strong cohesion and a polymeric matrix – provides a dense physical barrier against cell exposure to NPs; abundant EPS in the aggregate matrix entrap NPs near the outside of aggregates, thus protecting microorganisms residing in the interior. On the other hand, adaptation mechanisms such as the proliferation of resistant individual strains, community resilience (understood as the ability to counteract antimicrobial action with increased microbial growth) and functional redundancy (*i.e.*, the presence and prevalence of equivalent microbial functions to those provided by susceptible microorganisms) are accentuated by microbial diversity and social interactions within microbial aggregates [21].

The example of AGS technology, characterized by self-established, dense microbial aggregates, is therefore regarded as one of the most suitable solutions available for the treatment of Ag NP-loaded wastewaters. To date, however, only two published studies have been submitted with direct mentions to the subject. Gu *et al.* (2014) compared the removal of Ag NPs by flocculent and granular sludge as well as their short- (12 hours) and long-term (22 days) inhibitory impacts. Flocculent sludge proved better in terms of absolute Ag NP removal owing to the larger surface area of

sludge flocs, but was shown to be more susceptible to silver exposure, sustaining reductions in ammonia oxidizing rate when exposed to 1–100 mg Ag NPs L^{-1} for up to half a day and in specific oxygen uptake rates in the long run. Even though it proved less efficient in removing Ag NPs, AGS showed increased resistance in both time-frames, with no significant drops in either activity [22]. More recently, Quan *et al.* (2015) exposed two equivalent AGS systems to 5 and 50 mg Ag NPs L^{-1} for 69 days and evaluated the impacts of exposure over microbial activities, pollutant removal and sludge properties by comparison with a silver-free control. Both systems were able to operate with no significant reduction in activity until day 35, but experienced drops in the respiration, ammonia oxidizing and denitrification rates thereafter. Despite these setbacks, overall COD and ammonia removal efficiencies remained above 90% throughout the entire operation and no significant impacts seemed to bear over sludge settleability, granule architecture or community structure [23].

While promising as preliminary dashes into the feasibility of AGS treatments for Ag NP removal, these studies are limited in temporal scope and focus mainly on microbial activities to characterize toxicity. Longer operation times are required to clarify just how far silver dosing can go before reaching a retention limit or forcing the system into shutdown and a deeper focus on the micro- and microscopic parameters associated with granule stability is necessary to understand whether negative impacts are to be expected solely in association with microbial activities. Moreover, clarifying the ways in which bioreactor operation can impact on silver toxicity is required if negative effects are to be averted. In order to answer some of these questions, this study used two SBRs with different operating parameters known to impact on sludge properties (namely shear stress and feeding strategy) and investigated the bearings of persistent silver dosing at 10 mg Ag NPs L^{-1} on bioreactor operation for 192 days.

Materials and methods

Synthetic textile wastewater

Carbon source and azo dye stock solutions. Emsize E1 (Emsland-Stärke GmbH, Germany), a starch derivative (hydroxypropyl starch) used as a sizing agent in the cotton textile industry, was used as carbon source for the preparation of the synthetic textile wastewater. Under the alkaline conditions applied in the desizing step of cotton manufacturing, Emsize E1 is hydrolysed and released in the effluent. The preparation of the stock solution (100 g L^{-1}) was based on one set of desizing conditions provided by the manufacturer. Briefly, 100 g of Emsize E1 and 40 g of sodium hydroxide were dissolved in distilled water and stirred for 15 hours at room temperature. The hydrolysed solution was then neutralized to pH 7.0 $\pm$ 0.05 with 37%(m/m) HCl and diluted to 1 L with distilled water.

The azo dye stock solution (5.0 g L^{-1}) was prepared by dissolving Acid Red 14 (AR14; Chromotrope FB, 50% dye content, Sigma-Aldrich Química, S.L., Portugal) in distilled water.

Synthetic wastewater composition. The synthetic TWW used as a feed solution was prepared by diluting the carbon source to a COD content of 1,000 mg O_2 L^{-1} (1.15 g L^{-1} Emsize E1) and the azo dye to a final concentration of 40 mg L^{-1}. Each component was added from equal volumes of two separate concentrated solutions containing the carbon (Feed C) and nitrogen sources (in the form of ammonium chloride; Feed N), and supplemented with macro- (magnesium, calcium, and iron salts) and micronutrients (manganese and zinc sulphates, boric acid, and ammonium molybdate) respectively. pH buffering phosphates were added to the final wastewater along with the remaining components of Feed N to produce an influent COD:N:P mass ratio of 100:3.7:37. The final composition of the simulated wastewater was as follows: 2,310 mg L^{-1} $Na_2HPO_4{\cdot}12H_2O$, 762 mg L^{-1} KH_2PO_4, 143 mg L^{-1} NH_4Cl, 27.5 mg L^{-1} $CaCl_2$, 22.5 mg L^{-1} $MgSO_4{\cdot}7H_2O$, 250 μg L^{-1} $FeCl_3{\cdot}6H_2O$, 40 μg L^{-1} $MnSO_4{\cdot}4H_2O$, 57 μg L^{-1} H_3BO_3, 43 μg L^{-1} $ZnSO_4{\cdot}7H_2O$, and 35 μg L^{-1} $(NH_4)_6Mo_7O_{24}{\cdot}4H_2O$. Reported concentrations represent net inlet loads after dilution with an Ag NP suspension fed separately to the SBRs according to a 4:1 (other components:Ag NP) volume ratio. All salts were analytical grade.

Silver nanoparticle suspension. Ag NPs with a maximum particle size of 100 nm (with added polyvinylpirrolidine as dispersant) were purchased as a powder from Sigma-Aldrich Química, S.L. (Portugal). Silver nanoparticle stock suspensions (100 mg L^{-1}) were prepared by dispersing 200 mg Ag NPs in 2 L of MilliQ water and stabilized by ultrasonication on ice (150 W, 20 kHz) for 30 minutes using a Sonoplus HD 3200 ultrasonic homogenizer (Bandelin, Germany). The suspensions were fed to the SBRs from a top inlet port over a 15-minute period simultaneous with the introduction of fresh simulated textile wastewater.

Sequencing batch reactor (SBR) operation

Setup and basic operational parameters. Two non-tubular bubble column SBRs with a working volume of 1.5 L and a height-to-diameter ratio of 2.5, SBR1 and SBR2, were seeded with conventional activated sludge harvested from a full-scale municipal wastewater treatment plant in Chelas, Lisbon (Portugal), and operated in parallel for 192 days. The reactors were run in 6-hour cycles comprising five individual stages – fill, reaction (which included a mixed anaerobic stage and an aerobic stage), settling, drain, and idle – with a volumetric exchange ratio of 50% and a hydraulic retention time of 12 h. At the beginning of each cycle, synthetic TWW was fed in static and anaerobic conditions from the bottom of the reactors according to a volumetric organic loading rate of 2.0 kg COD m^{-3} day^{-1} using one of two different strategies: an uprising plug flow developed from the centre bottom and spread out through the sludge bed (in SBR2), or a rapid discharge at a peripheral site followed by a fast and channelling rise across the settled biomass (in SBR1). Towards the end of the filling stage, 150 mL of a concentrated Ag NP suspension (100 mg L^{-1}) were added from the top of the reactors to produce an added silver concentration of 10 mg L^{-1} at the onset of the reaction phase.

Sequencing batch cycles were timed to include 30 and 60 minutes of anaerobic feeding in SBR1 and SBR2 respectively, followed by a stirred anaerobic phase stretching to the 2-hour mark (*i.e.*, 1.5 h in SBR1 and 1 h in SBR2) and a 3.5-hour aeration period. Mechanical mixing was provided by a magnetic anchor impeller (ϕ = 6 cm) at 70 rpm in SBR1 and by a pitched-blade turbine (ϕ = 5 cm) at 280 rpm in SBR2. During the aerobic stage, fine bubble diffusers installed at the bottom of the reactors and connected to air compressors (SPP-20GJ-L, Hiblow, Japan) provided aeration at a flow rate of 2 vvm. After settling, supernatant withdrawal was performed over 1 minute and the reactors were left in a quiescent state until the start of the next cycle. The operation was conducted at room temperature with no pH control and sustained pH variations in the 6.1–6.9 range along each cycle. All pumping, aeration and agitation functions were automatically controlled via an interface by a dedicated software installed in a personal computer.

Inoculation and aerobic granulation. SBR1 and SBR2 were seeded with 1.30 and 1.50 g TSS L^{-1} of CAS, respectively, and operated during the first 3 days with a settling time of 60 minutes so as to minimize biomass wastage and provide a suitable adaptive period to the new feeding conditions. Aerobic granulation was induced by applying progressively smaller settling times, high hydrodynamic shear stresses, and a feast-famine regime for biomass culture. The sedimentation time was shortened in a

stepwise manner during the first 4 weeks of operation in order to select fast-settling sludge particles, starting at 40 minutes (days 3–7) and going down to 30 min (days 7–10), 20 min (days 10–14), 15 min (days 14–17), 10 min (days 17–24), 7 min (days 24–28) and 5 min (from day 28 onwards). The final step reduction defined a minimum settling velocity of 1.5 m h^{-1} for biomass retention throughout the remaining operation time. Settling periods larger than 15 min were accommodated by reducing the aeration time accordingly in order to maintain a total cycle time of 6 hours. Feast-famine conditions were developed by allotting a relatively short feeding period and promoting a rapid consumption of the carbon source during the mixed anaerobic stage, thereby limiting the externally available COD for the remainder of the cycle time. The required shear stress was achieved by mechanical mixing during the anaerobic phase (described by a maximum tip speed of 26 and 88 m min^{-1} in SBR1 and SBR2, respectively) and by aeration during the aerobic phase (described by an upflow air velocity of 0.4 m min^{-1} in both reactors).

Analytical methods

Physicochemical parameters. Total suspended solids (TSS), volatile suspended solids (VSS), COD and pH were determined according to standard procedures [24]. Sludge volume index (SVI) was determined by measuring the volume occupied by the sludge settled from 1 L of mixed liquor after settling times of 5 and 30 minutes in an Imhoff cone (SVI_5 and SVI_{30}, respectively), and dividing it by the mixed liquor TSS value. Biomass morphological analysis was carried out using a transmission light microscope (BA200, Motic) fitted with a digital camera and respective software (Moticam 2, Motic). The proportion of large granules (sizes above 0.65 mm), small granules (sizes within the 0.2–0.65 mm range) and flocs (sizes under 0.2 mm) in the SBRs was estimated by sieving mixed liquor samples through 0.65-mm and 0.2-mm net sieves and determining the biomass content in each collected fraction using the TSS analysis protocol.

Colour removal was evaluated spectrophotometrically by tracking mixed liquor absorbance at 515 nm (the wavelength of maximum absorbance in the visible range by AR14) using a Specord 200 spectrophotometer (Analytik Jena, Germany). UV-visible absorption spectra were plotted for all collected samples in order to validate the mechanism of colour removal and track the accumulation and conversion of aromatic amines. Reporter wavelengths were selected from the absorption spectrum of a standard solution of the aromatic amine 4-amino-naphtahlene-1-sulphonic acid (4A1NS, Fluka, USA), one of the constitutive moieties of AR14 admitted to result from the reductive cleavage of the azo bond. Amine conversion was evaluated in terms of percent reductions in the absorbance of the mixed liquor at the chosen wavelengths during the aerated reaction stage. All absorbance measurements were performed against a distilled water blank.

N-*acyl-L-homoserine lactone-based QS analysis.* To assess the impact of QS mechanisms during granule formation and maintenance, AHL contents were evaluated weekly in sonicated and clarified AGS extracts using a microplate colorimetric biosensor assay. The assay involved (*i*) the AHL-mediated synthesis of *β*-galactosidase in reporter strain *Agrobacterium tumefaciens* NTL4(pZLR4) and (*ii*) the measurement of hydrolytic activities with chromogenic substrate X-gal [25]. The biosensor strain was grown at 28 ºC with orbital shaking (150 rpm) for 16–18 hours in AT minimal medium (10.5 g L^{-1} K_2HPO_4, 4.5 g L^{-1} KH_2PO_4, 2 g L^{-1} $(NH_4)_2SO_4$, 200 mg L^{-1} $MgSO_4 \cdot 7H_2O$, 15 mg L^{-1} $CaCl_2 \cdot 2H_2O$, 10 mg L^{-1} $FeSO_4 \cdot 7H_2O$, 3 mg L^{-1} $MnSO_4 \cdot H_2O$) containing 0.2%(w/v) glucose and 50 μg mL^{-1} of gentamicin. Seed cultures were diluted to an optical density at 600 nm (OD600) of 0.02 using fresh minimal medium (without antibiotics) and supplemented with X-gal (250 μg mL^{-1}) to produce the AHL bioassay solution. 15 μL of cell-free AGS extracts were mixed with 235 μL of this solution in 96-well plates and incubated in the dark with gentle shaking for 13 hours using a Stat Fax-2200 shaker-incubator (Bio-Rad, USA) at 28ºC. Cell-density normalized activity levels were determined in the final biosensor cultures using dual-wavelength optical density readings [25] and expressed as nmol-equivalents of the reference AHL *N*-(3-oxododecanoyl)-L-homoserine lactone ($3OC12\text{-}HSL_{eq.}$).

Statistical analysis

Statistical analyses were performed using Excel® (Microsoft, USA) and GraphPad Prism 6 (GraphPad Software, USA). One-way analysis of variance (ANOVA) with Holm-Šidák post-test was conducted to examine differences in equivalent 3OC12-HSL concentrations along the operation of each reactor and adjusted *p*-values are reported. Multiple unpaired *t*-tests were used to compare weekly results of AHL-based quorum sensing in between the two SBRs and family-wise error rate corrections were provided using the Holm-Šidák method (adjusted *p*-values are reported).

Results and Discussion

Biomass properties, inventory and morphology

Sludge morphology and granule size distribution. The CAS inoculum – which consisted mostly of small, pinpoint flocs (94% of mixed liquor TSS) – successfully aggregated to form granular structures during the first 16 days of operation in both SBR1 and SBR2. Along this period, the proportion of small granules significantly increased in both SBRs, while the large granular fractions saw a small increase in SBR1 (from 1.1 to 1.9%) and a slight reduction in SBR2 (from 1.1 to 0.7%) (Fig. 1A). The collapse of biomass aggregates with large diameters in SBR2 might be associated with the use of a higher stirring speed during the mixed anaerobic stage (280 rpm, as compared to 70 rpm in SBR1) and interpreted as a consequence of (*i*) higher hydrodynamic shear forces near the impeller, promoting sloughing or disruption of large granules; and (*ii*) higher fluid and sludge circulation velocities, resulting in stronger attrition upon collision of biomass particles. Despite the successful development of aerobic granules in both systems, biomass aggregation seemed to occur at a faster rate in SBR1 along the first two weeks of operation, resulting in granular fractions of 11% on day 16 as compared to 7.8% in SBR2 (Fig. 1A). Once again, the governing mixing conditions in SBR2 might be invoked as one of the main reasons for this evolution and associated with an operational counterbalance between the drive between the drive for microbial agglomeration and the application of strong dispersive shear forces.

After the initial aggregation stage both SBRs experienced granule breakup episodes that resulted in the disruption of either all or most large aggregates and in reduced overall granular fractions (d > 0.2 mm) – 4.5 and 2.0% in SBR1 and SBR2, respectively, on day 59 (Fig. 1A). The most significant drop in the proportion of granules was recorded between days 16 and 30 (Fig. 1A), suggesting an early loss in granule stability during a stage of the operation where settling times were continually reduced to foster the development of mature aerobic granules. Interestingly, several small light-coloured aggregates with even outlines, likely containing high concentrations of bound extracellular polymeric substances (EPS), were seen in combination with the biomass in both bioreactors between days 22 and 52 (Fig. 1B), reflecting the presence of bacterial strains with high EPS-producing capacities despite the tendency for granule disintegration. The combined weight of these observations can provide some context for the causes of AG disruption. In fact, intensive EPS production has been suggested by a number of authors to result in the clogging of granule pores, causing restrictions in the transport of substrates

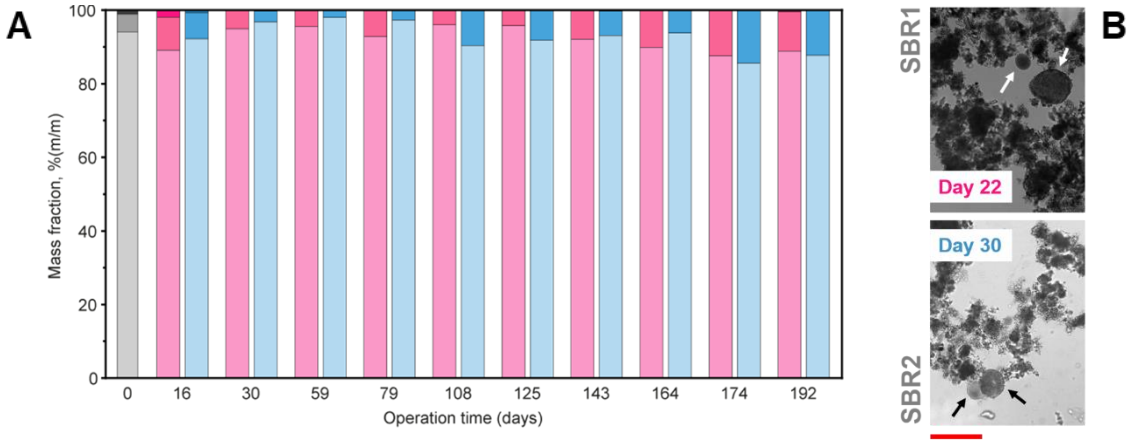

Figure 1 | Biomass particle size distribution (in terms of mass fraction) and important traits of sludge morphology. (A) Comparison between the mass fraction of sludge flocs (■,■,■; d < 0.2 mm), small granules (■,■,■; 0.2 mm < d < 0.65 mm), and large granules (■,■,■; d > 0.65 mm) in the CAS inoculum (grayscale), in SBR1 (pink gradient), and in SBR2 (blue gradient). (B) Transmission light micrographs – 100x magnification – of biomass samples collected from SBR1 (top) and SBR2 (bottom) highlighting the presence of light-coloured EPS-rich aggregates after day 22; scale bar (in red, bottom): 250 μm

and metabolites into and out of the EPS matrix and often leading to cell death in the inner layers – through starvation or prolonged exposure to toxic by-products [26,27]. Over time, this phenomenon can destabilize the AG core, causing the structure to become brittle and eventually leading to the disruption of the granular architecture [27,28]. The heightened EPS producing capacity developed in SBR1 and SBR2 during these early stages could therefore have impacted negatively on AG stability, causing disintegration and motivating a sharp drop in granular fractions.

From day 59 on, granular structures in SBR1 and SBR2 were partially and slowly recovered up until the end of the operation (on day 192), following distinct patterns in each bioreactor. In SBR1, the proportion of aerobic granules initially surged (from day 59 to day 79), but subsequently declined back to stable levels at approximately 4%. From day 125 onwards, biomass aggregation promoted the development of a large number of small granules, which accounted for 10.7% of the total sludge mass by day 192. In SBR2, granular fractions increased from 2.7 to 9.6% between days 79 and 108 only to decrease slowly over the course of the following eight weeks; during the final month of operation (from day 164 onwards), the bioreactor quickly accumulated small granules up to a final mass fraction of 12% (Fig. 1A). Amid these successive restructuring and breakup episodes, granular fractions in SBR2 overtook those of SBR1 on day 108 and then again on day 174, thereby proving the influence of factors other than hydrodynamic shear in dictating the comparative edge between the granulation grade of the two systems.

Sludge settleability and biomass inventory. Evolutions in sludge settleability and biomass concentrations during the first 4 weeks of operation progressed displayed some similar trends in SBR1 and SBR2. Following an initial drop in SVI_5 and SVI_{30} values during the first week of operation (Fig. 2A), both systems embarked on a stage of sludge build-up that raised mixed liquor VSS contents (MLVSS) to local maximum levels of 6.2 g L^{-1} in SBR1 (on day 24) and 4.6 g L^{-1} in SBR2 (on day 21) (Fig. 2B). The described growth curve can be interpreted as a reflection of the good biomass retention capacity in the bioreactors and correlated with the development of fast-settling aerobic granules throughout the first two weeks of operation (consistent with the results from sieving analysis; Fig. 1A). Despite this initial evolution, however, both sludge systems proved sensitive to the increasing hydraulic selection pressure, recording severe washout events from day 17 on that brought biomass accumulation to a halt (Fig. 2B). In the wake of these washout events, SVI_5 and SVI_{30} values dropped further still, reaching 78 and 47 mL g^{-1} MLTSS in SBR1 and 97 and 61 mL g^{-1} MLTSS in SBR2 on day 31 (Fig. 2A) and reflecting the removal of slow-settling biomass particles. Similarities notwithstanding, evolutions in MLVSS and SVI levels in SBR2 throughout this period were much more measured and hint at a gradual formation of AGs that offers some context to the comparative superiority – in terms of granular fractions – of SBR1 along the initial leg of the operation

Beyond the final settling time reduction, SVIs continued to decrease in both SBRs despite the evidence for granule disruption between days 16 and 59 (Fig. 2A). In response to the improvement in sludge settleability, biomass accumulated once again until day 50, reaching maximum concentrations of 8.2 g VSS L^{-1} in SBR1 (on day 56) and 6.8 g VSS L^{-1} in SBR2 (on day 50) (Fig. 2B). The comparatively higher levels achieved in SBR1 during this stage and throughout most of the experimental run are the product of inferior SVI values that allowed the bioreactor to retain a more compact sludge system with superior microbial concentrations and are, once again, a likely result of the lower shear conditions imposed in the bioreactor [29]. Effluent VSS concentrations measured after day 28 significantly declined when compared to the levels of previous days and were maintained at around 100 mg VSS L^{-1} until day 56 (Fig. 2B). As a result, sludge retention times (SRT) increased to maximum values of 40 days in SBR1 (on day 50) and 38 days in SBR2 (on day 38) throughout this period (data not shown).

Following this accumulation stage, biomass concentrations reached the maximum retention capacity of the bioreactors and stagnated around the previously mentioned maxima for several weeks – between days 44 and 56 in SBR1 and between days 50 and 70 in SBR2 (Fig. 2B). Throughout this period, sludge settling properties underwent a gradual deterioration that progressed until day 85 to reach local maximum levels in SBR1 (SVI_5 and SVI_{30} values of 103 and 66 mL g^{-1} MLTSS) and SBR2 (SVI_5 and SVI_{30} values of 122 and 77 mL g^{-1} MLTSS) (Fig. 2A). As a result, two intense periods of biomass washout recorded between days 63 and 85 caused MLVSS contents to drop steeply from their plateaus to local minima of 4.4 mg L^{-1} in SBR1 (day 70) and 4.1 mg L^{-1} in SBR2 (day 85) (Fig. 3B). This episode marked the beginning of a long period of dynamic changes in sludge properties that progressed, with only minor distinctions between the two bioreactors, according to mirror images in the SVI and MLVSS profiles. The recorded evolution is best subdivided in the following three stages (Fig. 2):

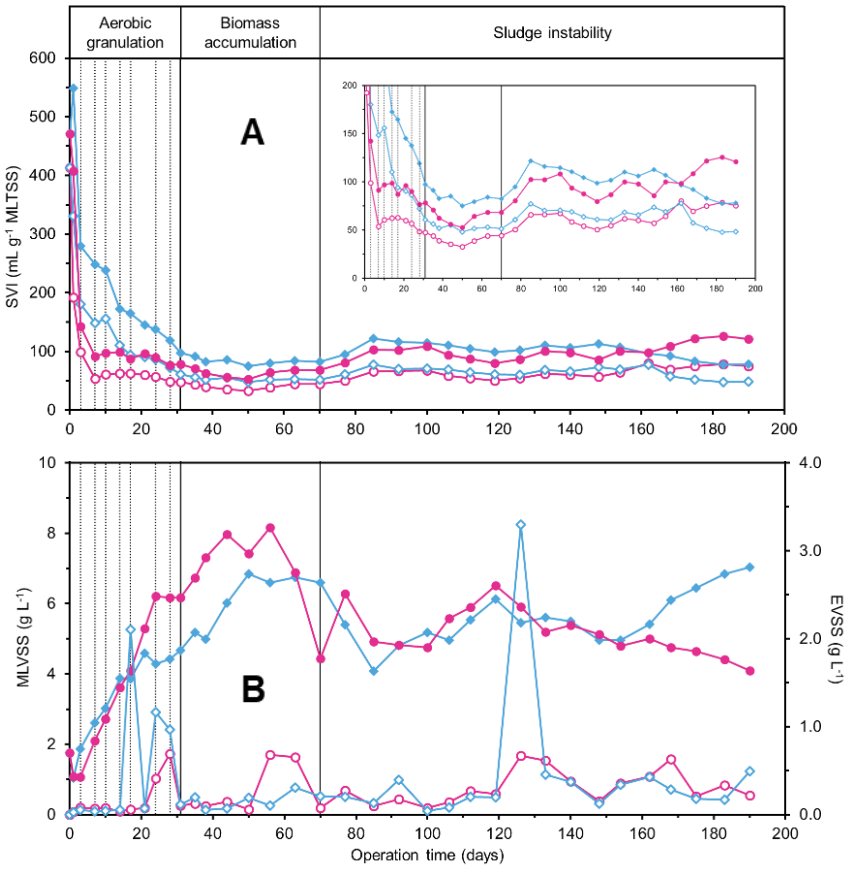

Figure 2 | Sludge volume indexes (SVI) and biomass concentration along the experimental run. (A) SVI values measured after a 5-minute settling period (SVI_5) in SBR1 (●) and SBR2 (◆), and after a 30-minute settling period (SVI_{30}) in SBR1 (○) and SBR2 (◇). The inset plot displays a focused profile for SVI ≤ 200 mL g^{-1} MLTSS. (B) Volatile suspended solids contents in the mixed liquor (full symbols) and in the effluent (open symbols) from SBR1 (●,○) and SBR2 (◆,◇). Vertical dotted lines on the left-hand side denote the days where step reductions in settling time were applied.

(i) a paced sludge accumulation between days 85 and 119 driven by gradually decreasing SVI_5 and SVI_{30} values (effective in SBR1 only from day 100 on); peak MLVSS contents were recorded on day 119 at 6.5 and 6.1 g L^{-1} in SBR1 and SBR2, respectively;

(ii) a reversal of the previous progress, characterised by heavy biomass washout after day 126 and stretching until day 148 (when comparable MLVSS levels of ~5.0 g L^{-1} were reached in both systems);

(iii) a period of divergence from day 148 on to the end of the operation, characterised by an improvement in sludge settleability in SBR2 and by increasing SVI values in SBR1; as a result, biomass concentrations increased in the former case (up to 7.0 g L^{-1}) and decreased in the latter (down to 4.1 g L^{-1}); this final period marks the only instance of the whole experimental run where SVI and MLVSS levels in SBR2 surpassed those of SBR1.

These episodes follow multiple variations in the mass proportion of granules in the sludge bed (as revealed by sieving analysis) that relate differently to sludge settleability in each reactor. In the case of SBR2, the succession of granule formation and breakdown events previously inferred in Fig. 1A concurs with the SVI profiles in describing a stage of granule restructuring concomitant with the progressive improvement in sludge settleability recorded between days 85 and 119 (SVI_5 and SVI_{30} values of 99 and 61 mL g^{-1} MLTSS down from 122 and 77 mL g^{-1} MLTSS). Following this period, the final fast granulation phase led to a similar decrease in SVI values (from day 148 until the end of the operation) that further validates a correlation between the two variables. The same is, however, not true for SBR1. These results suggest that, beyond the first few weeks of operation, where sludge aggregation resulted in dense structures that significantly reduced SVI values, biomass flocs in SBR1 aggregated to form aerobic granules with poor settling properties.

Contradictory short- and long-term impacts of Ag NP dosing. Ag NPs seemed to exert no significant negative impact over the process of aerobic granulation proper despite the high influent concentration (10 mg L^{-1}), with both bioreactors recording significant improvements in sludge settleability over the first 50 days and going on to form granules unhindered. Previous studies conducted in our lab have demonstrated that silver nanoparticle loadings as high as 5 mg L^{-1} similarly bear no influence on the dynamics of aerobic granulation [30,31], which indicates AG formation is – at least along the tested loading range – relatively impervious to the antimicrobial action of Ag NPs. This sort of behaviour suggests that all relevant microbial functions involved in granulation could be maintained inside the bioreactors even after exposure to Ag NPs. Results from a recent study conducted with activated sludge have demonstrated that, contrary to expectations, relatively low doses of Ag NPs (1 mg L^{-1}) – especially freshly prepared Ag NPs – can actually help maintain or even increase the diversity and functional richness of the microbial community and thus contribute to increase its resistance in the event of further toxic shocks. The same study also documented an improvement in sludge settleability and a consequent increase in biomass concentrations after exposure [3]. This sort of constructive spur in response to low concentrations of a toxicant is called a hormetic effect and has been reported in a number of other studies investigating the impacts of Ag NP dosing in both defined planktonic and biofilm cultures [32,33]. In light of these results, the presence of Ag NPs in SBR1 in SBR2 during the initial stages of the operation might actually have contributed productively for some of the developments in AG formation, settleability and biomass accumulation, helping in the establishment of the AGS system.

Sludge property developments recorded form day 70 onwards appeared, however, to reveal a destabilizing effect lurking behind the constant addition of Ag NPs. As described above, right after the bioreactors reached their respective sludge retention thresholds, dramatic washout events on day 85 resulted in the removal of nearly half the resident biomass and initiated a period of cyclical sludge accumulation and sludge removal – accompanied by improvements and decays in settleability (Fig. 2). These patterns are at least partly in line with SVI and MLTSS profiles plotted for SBR1 in a previous operation carried out with a nominal Ag NP load of 5 mg L^{-1} by Bento (2016), where a sharp drop in biomass concentrations could be detected few weeks after sludge accumulation ceased. The bioreactor was operated against an identical, Ag NP-free control that displayed no similar washout event, indicating a direct association between biomass removal and silver dosing [30]. The combination of these results seems to suggest that Ag NP accumulation in the bioreactors can occur with minor harm to the operation up to a given limit before negative

impacts emerge. Biomass washout resulting from the violation of this limit results in a reduction of accumulated nanoparticle contents and effectively initiates a new stage of the cycle where sludge properties improve continuously until the threshold is exceed again. Similar conclusions were advanced by Sheng et al. (2018), who noted a decay in sludge settleability and biomass retention capacity 40 days into the operation of a CAS SBR exposed to fresh Ag NP suspensions despite initially positive developments. The bioreactor was stopped before severe washout events could be recorded and the cycle could be repeated, but Ag NP accumulation was equally suggested as the main causative factor [3].

This behaviour emerges as a consequence of the prime retention capacity of AGS reactors, seeing as sludge particles are allowed to remain in the system over extremely long periods of time, continually interacting with and amassing inbound nanoparticles. Control strategies aiming to limit Ag NP accumulation in these systems (or any other bioreactor designs characterized by high retention) should therefore be devised whenever consistently high NP loadings are expected. Periodical biomass removal for SRT control is one possible solution with a long track record in the context of wastewater treatment and could prove sufficient to avoid operational instability.

Long-term impacts of anaerobic feeding strategy on sludge properties. As previously mentioned, despite the evidence for granule reformation recorded in both bioreactors towards the end of the experimental run, sludge settleability in the two systems was seen to follow, after day 148, two inconsistent trends that hint at the accumulation of dense structures with high settling velocities in SBR2 and at the presence of low-density granules with poor sedimentation ability in SBR1 (Figs. 1 and 2). These results contrast significantly with settleability trends identified throughout the remaining operation time and signal the influence of some factor other than hydrodynamic shear in defining the balance of macroscopic sludge properties. While no independent measurement performed throughout the experiment can be used to clearly establish what this factor was, the particularities of each system's anaerobic feeding strategy could be advanced as likely contenders. Causation links between feeding and these observations emerge in association with each system's characteristic fluid circulation patterns across the sludge bed and could result from different biomass concentrations inside the granules – as previously suggested by Franca *et al.* (2017) in a different operation with the same bioreactors [19].

The use of a plug-flow hydrodynamic regime (as applied in SBR2) rising through the settled sludge bed, with a high substrate concentration, allows soluble, easily biodegradable substrates to penetrate the entire AG depth and be converted to storage polymers by relevant PAO and GAO populations. These storage polymers can subsequently be used as carbon and energy sources over the course of the aerobic phase, sustaining slow microbial growth down to the granule core and ensuring the development of a stable, dense structure. Conversely, by limiting the contact of the influent feed solution with the settled biomass, the fast, static filling arrangement imposed in SBR1 leaves the bulk of substrate consumption for the subsequent anaerobic mixed phase and forces AGs to contact with a diluted substrate – mixed in with the leftover effluent from the previous cycle [19]. As a result, storage polymer reserves accumulated under anaerobiosis might prove insufficient to secure basic maintenance functions during the aerobic phase, leading to cell death and to the creation of empty pockets inside the granular volume that contribute for a light structure. Granules grown in SBR1 by Franca *et al.* (2017) were indeed shown to display sparse storage polymer reserves towards the end of the reaction cycle [19] and could serve as models for the AGs obtained during this work.

Treatment performance

COD removal performance. The overall COD removal yields obtained along the experimental run are represented in Figure 3 together with the fraction of the overall yield that was removed (*i*) during plug-flow filling in SBR2 and (*ii*) by the end of the anaerobic mixing phase in both reactors. Conversion during the fast, static filling stage imposed in SBR1 was deemed negligible (data not shown) and is therefore not represented; as such, removal yields for the bioreactor are defined by comparison with the COD content assayed at the onset of the stirred anaerobic phase.

As depicted, overall COD removal levels remained below the 50% mark during the first week of operation, likely due to the change in the main carbon substrate from domestic wastewater to the synthetic textile effluent with hydrolysed hydroxypropyl starch as carbon source. However, the microbial communities in the bioreactors efficiently adapted to the new carbon source, reaching COD removal yields of 70 and 75% on day 14 (in SBR1 and SBR2, respectively), and subsequently stabilizing in the 80–90% range (with occasional drops) from day 38 on – despite the continuous loading of Ag NPs and the observed shifts in granulation grade, biomass concentration, and sludge settleability. The absolute COD removal capacity of the bioreactors reached a steady state on day 17, limiting the consumption of organic matter up to residual levels in the 50–110 mg O_2 L^{-1} range. Conversely, carbon load removal yields during the anaerobic stage saw significant variations throughout the operational run. Relative conversion during plug-flow filling in SBR2 varied between −14% (days 38 and 162) and 49% (day 126) according to a mostly random pattern, a result that could be ascribed to the non-tubular geometry of the bioreactor. As previously stated, low H/D ratios have previously been shown to hinder proper influent distribution across the settled sludge bed during plug-flow feeding by promoting random channelling routes. The random nature of these channels induces marked variations on the effective contact time between the biomass and the influent solution, steering the fluid through longer or shorter paths from cycle to cycle and thus causing COD conversion yields to oscillate profusely [18].

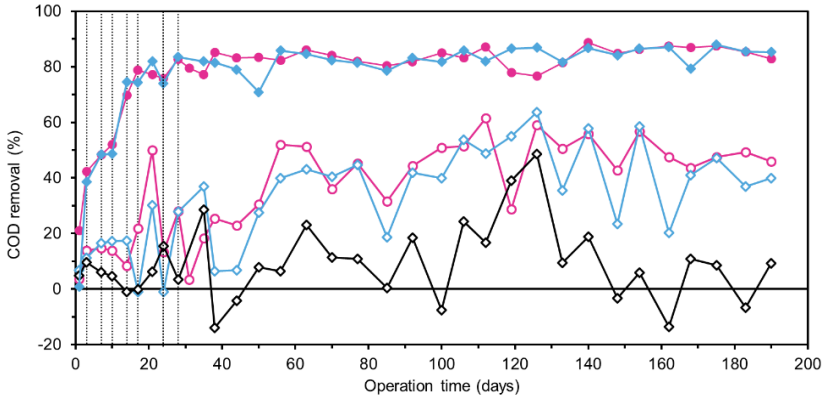

Figure 3 | COD removal performance along the experimental run. Relative anaerobic (○,◇) and overall COD removal yields (●,◆) in SBR1 (pink) and SBR2 (blue), plus the partial relative contribution attributable to plug-flow filling in SBR2 (◇). Vertical dotted lines on the left-hand side denote the days where step reductions in settling time were applied.

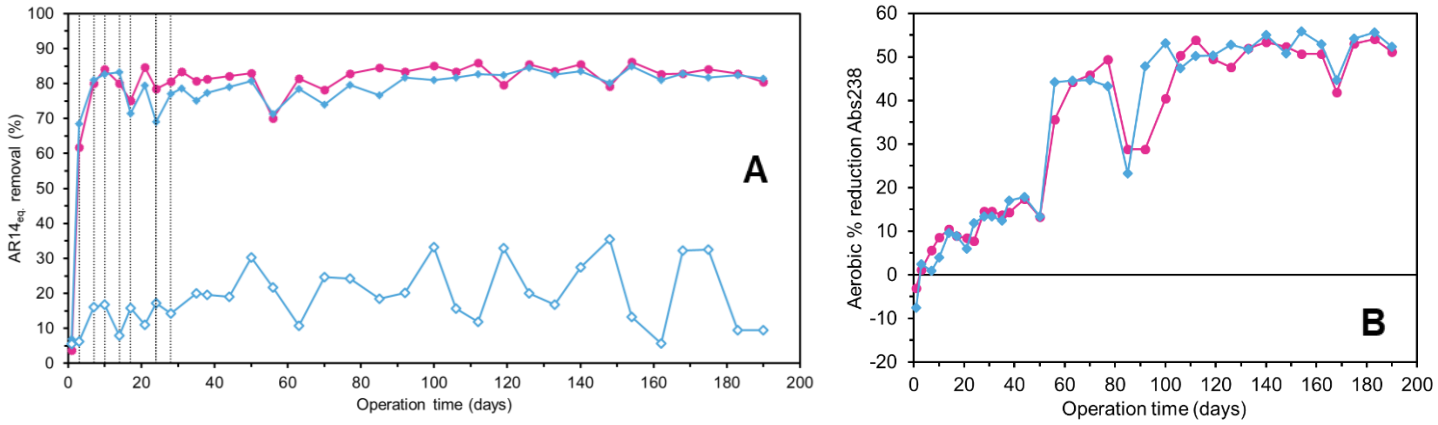

Figure 4 | Colour removal performance and apparent aromatic amine conversion along the experimental run. (A) Overall colour removal yields in SBR1 (●) and SBR2 (◆) and percent reduction in $AR14_{eq.}$ during the plug-flow feeding stage of SBR2 (◇). Vertical dotted lines on the left-hand side denote the days where step reductions in settling time were applied. (B) Percent reduction in mixed liquor absorbance at (A) 218 nm, (B) 238 nm, and (C) 318 nm during the aerobic reaction period of SBR1 (●) and SBR2 (◆)

While less inconsistent, trends for the partial anaerobic COD removal yields were also seen to vary along the operation. By conflating carbon removal patterns with pH curves plotted individually for each sampled cycle, some of these variations could be seen to reflect an evolution in the resident sludge community's ability to degrade the incoming substrates anaerobically while others were concluded to emerge from changes in feed composition prior to feeding (data not shown). In general, however, anaerobic COD consumption described a rising trend over the course of the operation – peaking at 62% and 64% in SBR1 and SBR2, respectively – that points to a gradual proliferation of anaerobic heterotrophs. Likewise, pH curves revealed a decreasing trend during the anaerobic stage of most sampled cycles (data not shown) that is consistent with the accumulation of volatile fatty acids in the mixed liquor and might be regarded as indirect evidence of a significant fermentative activity within the microbial community. Sludge washout episodes recorded during the first few weeks (as a result of settling time reductions) and later on in the operation (around day 85 and after day 119) seemed to motivate concomitant drops in the anaerobic contribution for carbon removal, suggesting important bacterial activities were removed from the bioreactors as a consequence. In associating these results with previous conclusions regarding the role of Ag NP accumulation as a driver of sludge instability and a trigger for biomass washout, silver nanoparticle dosing might be regarded as one of the ultimate causative factors behind these drops in anaerobic COD removal.

Colour removal and aromatic amine conversion. Figure 4A provides a breakdown of overall colour removal yields obtained in SBR1 and SBR2 throughout the operation, along with the fraction of the overall yield removed during the plug-flow feeding stage of SBR2. As with results from COD analysis, decolourization yields computed for SBR1 were defined in reference to mixed liquor colour contents measured at the onset of anaerobic mixing and disregard residual contributions originating in the filling stage (shown to amount to less than 10% of the nominal initial AR14 concentration; data not shown).

As depicted, AR14 conversion during filling in SBR2 varied from a minimum of 5.6% on day 1 to a maximum of 35% on day 140 with significant oscillations along the experimental run that occurred randomly and according to no obvious relation with the remaining shifts in sludge properties. These results are once again easy to perceive as the direct consequence of an imperfect plug flow forming channels across the sludge bed and causing the effective sludge/influent contact time to vary from cycle to cycle.

Outside the filling phase, the resident sludge community in the bioreactors appeared to adapt rapidly to the synthetic textile effluent, providing AR14 removal levels of 80% after only 7 days of operation. During the initial step reductions in settling time, colour removal yields suffered isolated drops in SBR1 (days 14, 17 and 24) and SBR2 (days 17 and 24) following discrete washout episodes that likely resulted in the removal of bacterial species with an azoreductase activity. From day 28 onwards, however, removal yields stabilized in the 74–86% range. These levels are similar to those from previous studies conducted in silver-free AGS systems treating synthetic textile wastewaters with identical compositions [1,8] and suggest the continuous feeding of Ag NPs had no relevant impact over decolourisation performance. The multiple washout episodes registered throughout the operation also seemed to produce no meaningful changes in AR14 removal, signalling the upkeep of a high azo dye-degrading capacity independently from sludge age restrictions; this can be attributed to the prime sludge retention capacity of the AGS SBR systems, which was able to ensure sufficient biomass concentrations to tackle the influent colour loading.

AR14 was shown to undergo reductive decolourization with azo bond cleavage by tracking the development of three characteristic peaks around the wavelengths of maximum absorption (218, 238 and 318 nm) of one of its constitutive aromatic amine moieties (4-amino-1-naphatalenesulfonic acid; 4A1NS). These same wavelengths were monitored throughout the length of the aerobic reaction stage in order to ascertain the bioreactors' ability to further convert the aromatic amine metabolites in the presence of oxygen. Figure 4B offers a summary of observed percent reductions in mixed liquor absorbance at 238 nm during the aerated phase and is provided as an example of a reporter variable for the quantification of 4A1NS conversion. Similar plots were derived for Abs reductions at 218 and 318 nm and yielded equivalent results.

As depicted, little changes in the absorption of the relevant wavelengths could be detected during the aerated reaction phase in either bioreactor along the first 50 days. However, between days 50 and 56 the reporter variable underwent sharp increases in both SBR1 and SBR2, signalling the proliferation of bacterial species with a capacity to metabolise 4A1NS. This result can be correlated with the progressive increase in sludge age observed along the first 50 days of operation [1,8,34] and might suggest that the development of an arylamine-degrading activity in the sludge community is intimately associated with slow-growing bacterial strains or with a selective effect brought about by the prolonged exposure to aromatic amines. While positive, in endorsing the

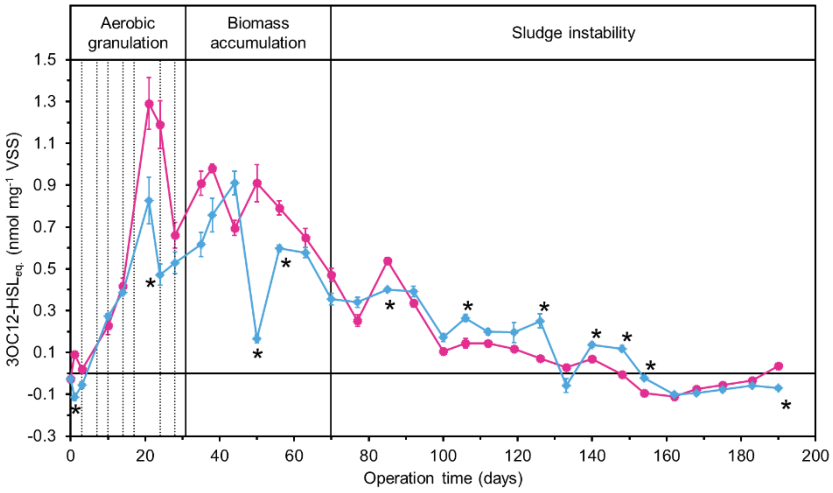

Figure 5 | Equivalent 3OC12-HSL concentrations, 3OC12-HSL$_{eq.}$, in cell-free AGS extracts collected along the experimental run. Variations in AHL levels – expressed in terms of the reference 3OC12-HSL – in SBR1 (●) and SBR2 (◆). The data were normalized to the respective sample biomass and are presented as the mean ± SEM of five or six independent replicates (cf. 2.5.4). Unpaired t-tests were conducted individually for every sampled day in order to compare the 3OC12-HSL$_{eq.}$ levels in each bioreactor. Significant differences ($p < 0.05$) are indicated by an asterisk next to the corresponding point in the profile of SBR2. Vertical dotted lines on the left-hand side denote the days when step reductions in settling time were applied.

benefits of high sludge ages these results emerge as a problematic blow to previous considerations on the use of short SRTs to abate the destabilizing effects of Ag NP accumulation in the sludge. Further studies investigating whether an adequate balance between structural stability and aromatic amine degradation can be reached in Ag NP-fed systems are therefore required.

Following the marked decrease in biomass concentration registered between days 77 and 85, aerobic percent reductions in UV absorption once again dropped to lower levels in both systems, signalling a loss of bacterial species with relevant activities for the conversion of 4A1NS, further backing the hypothesis of SRT mediation and once again hinting at a possible negative effect emerging from prolonged Ag NP dosing over the bioreactors' pollutant removal functions From this point on, however, the reporter variable rapidly climbed back to the levels attained before the washout event and seemed to remain approximately constant throughout the remaining operation time – showing an ability to maintain the aerobic aromatic amine degrading activity even in the long term.

AHL-based quorum sensing analysis

AHL contents in sludge extracts were evaluated in terms of the equivalent 3OC12-HSL concentration required to produce an equal normalized β-gal activity and subsequently corrected for sample biomass. The final results are expressed as 3OC12-HSL nmol-equivalents per milligram of volatile suspended solids, 3OC12-HSL$_{eq.}$, in Figure 5; significant differences between the levels examined in each bioreactor, as inspected by multiple unpaired *t*-tests, are marked with an asterisk. In the interest of clarity, adjusted *p*-values obtained for direct comparisons between the two SBR systems will hereinafter be represented by the symbol p_t. Results of the ANOVA performed individually for each bioreactor to track the evolution of AHL concentrations along the operation will similarly be backed, whenever relevant, by the corresponding *p*-values using the symbol p_A.

Aerobic granulation and biomass accumulation. Values of 3OC12-HSL$_{eq.}$ were observed to increase steeply in the first 21 days of operation from inoculum levels of -0.03 ± 0.02 (SEM) nmol mg^{-1} VSS to 1.2 ± 0.1 (SEM) and 0.8 ± 0.1 (SEM) nmol mg^{-1} VSS in SBR1 and SBR2, respectively ($p_A < 0.0001$ for both bioreactors). The observed evolution is consistent with the rapid development of aerobic granules recorded along the same period and suggests the existence of a direct association between granulation and AHL-based cell-to-cell signalling. These conclusions are consistent with those of previous studies demonstrating clear rises in sludge AHL contents during the early stages of granule development [10,13,35] and positive correlations between QS activity and microbial attachment potential [12]. The gap registered on day 21 between the 3OC12-HSL$_{eq.}$ levels of the SBR systems ($p_t = 0.3260$) suggests that the high hydrodynamic shear promoted during the mixed anaerobic stage of SBR2 exerted a deleterious effect over AHL quorum sensing and is largely consistent with previous observations regarding the presence of smaller granular fractions in SBR2.

After the peak levels of day 21, 3OC12-HSL$_{eq.}$ values dropped by 0.35 nmol mg^{-1} VSS in SBR2 on day 24 and by 0.63 nmol mg^{-1} VSS in SBR1 on day 28 ($p_A < 0.0001$ in both cases). These decreases follow two progressive reductions in settling time that could have resulted in the washout of AHL-producing bacterial populations and thus limited the concentration of signal molecules in sludge samples. Conceptual backing for this hypothesis can be found in the work by Tan *et al.* (2014), who reported concurrent variations in AHL content and the abundance of common AG community members with known QS activity [13]. As previously discussed, MLVSS and EVSS measurements performed throughout the final week of settling time reductions (Fig. 2B) seem to reflect a halt in the accumulation of biomass caused by the discharge of significant sludge volumes, and could thus offer some additional support to this hypothesis.

Despite the localized reduction, however, AHL contents in SBR2 described a rising trend following the definition of settling periods lower than 7 minutes, reaching peak levels of 0.91 ± 0.06 (SEM) nmol mg^{-1} VSS on day 44 (1.9 times higher than the minimum of day 24; $p_A < 0.0001$). Similar developments were registered in SBR1, with 3OC12-HSL$_{eq.}$ levels increasing by 0.32 nmol mg^{-1} VSS between days 28 and 38 ($p_A < 0.0001$) to reach a local maximum of 0.98 ± 0.02 (SEM) nmol mg^{-1} VSS. This evolution coincides with the detection of EPS-rich, light-coloured, round bacterial aggregates in the sludge systems of both bioreactors, and could point to an intimate relationship between AHL-based quorum sensing signalling and the production of high levels of bound extracellular polymeric substances. Correlations similar to this one have been established in previous studies by numerous authors [10,13,35] and suggested to act as one of the effective QS regulation mechanisms behind the process of aerobic granulation [36].

Long-term sludge maintenance. The local maximum 3OC12-HSL$_{eq.}$ levels recorded around day 40 were observed as a prelude to a period of approximately constant biomass concentrations in the bioreactors (starting on days 44 and 50 in SBR1 and SBR2, respectively; Fig. 2B) – consistent, as described above, with the respective maximum sludge accumulation thresholds. Throughout this period, AHL levels described a sharp descending drift, falling to below half their peak levels by day 70 ($p_A < 0.0001$ for both SBRs) and effectively reversing the rising trend of previous weeks. While several possible motivations for this evolution can be

invoked, regular biomass washout events along the MLVSS plateaus – with significant reductions in AHL-producing bacterial populations – are perhaps the most plausible candidates, backed in principle by the high EVSS levels recorded throughout (especially in SBR1; Fig. 2B).

After day 70, 3OC12-HSL$_{eq.}$ levels in SBR1 and SBR2 carried on decreasing from their initially high reaches, dropping to absolute minimum values on day 162 ($p_A < 0.0001$ in both systems for comparisons between the two dates). This evolution fared simultaneously with two surges in the proportion of granules in each sludge system (Fig. 1A) and seems to point both to a substantive divergence between granule reformation and AHL synthesis and to a lesser influence of QS mechanisms in the regulation of granule maintenance during the final leg of the operation. In trying to explain this trend, a look into the mechanisms of QS regulation working within the AG volume at different stages of the normal granule life cycle (preliminary aggregation → aerobic granulation → maturation → maintenance → decay) might prove insightful. Recent studies on the issue have established that microbial communities in AGs include both signal producers and microorganisms with quorum quenching abilities whose activities equilibrate to regulate environmental signal concentrations. The balance between the two communities is responsible for tuning interspecific and intraspecific communication inside the granule and can affect the sludge's structure and properties by controlling the expression of QS-based phenotypes related to granulation (such as EPS production) [37–39]. In analysing QS regulation during aerobic granulation, Tan *et al.* (2015) found a significant shift in the dominant species from potential signal quenchers to signal producers, underlining the role of species composition and associated signalling activities in coordinating community level behaviours [38]. Within the context of the current work, an opposite shift in the QQ-to-QS balance of the microbial community to that reported by Tan *et al.* (2015) [38] during long-term operation – promoting an increase in quenching activities and causing AHL levels to drop – might serve to justify the different 3OC12-HSL$_{eq.}$ values recorded in earlier and later stages of the experimental run. In agreement with this observation, Li *et al.* (2016) suggested that the proliferation of AHL quenchers and AHL producers in AGs is likely not synchronous, reporting a drop in AHL activity and diversity as granules matured and grew in size and finding consistent increases in the sludge's *N*-octanoyl-homoserine lactone-degrading activity over time [39].

Conclusions and future work

The impacts of Ag NPs over AGS properties, stability and treatment performance

The effects of silver nanoparticles on AGS stability were shown to be concentration-dependent, showing no apparent noxious action in the low concentration range but causing significant settleability decays and biomass washout when accumulated over long periods of time. In order to check whether these effects are avoidable, future studies could be designed to include periodic biomass withdrawals as a way of removing some of the accumulated silver and verifying sludge property evolutions.

Despite its impact on stability, Ag NP addition appeared to have no significant effect on the overall COD removal and decolourization abilities of either bioreactor, with relatively stable performance levels sustained at over 75% throughout the entire operation. Some secondary effects emerging in association with Ag NP-mediated destabilization could, nonetheless, be identified, specifically in terms of anaerobic COD removal (seen to drop on many an instance as a result of sludge washout) and, in one occasion around day 85, in terms of the apparent amine-degrading activity. These results suggest important bacterial activities can be eliminated if Ag NP toxicity is not curbed and advocate containment strategies that can limit silver accumulation in the biomass.

The effects of hydrodynamic shear and anaerobic feeding strategy over AGS properties and stability

Hydrodynamic shear proved important in defining the main macro- and microscopic properties of the sludge in the short-term horizon, with lower stresses promoting the development of AGS with better sludge settleability and facilitating granule growth. However, no apparent shear-associated effect could help steer biomass properties over the long run, with multiple incoherent variations in granulation grade and settleability taking place according to no set timing in either bioreactor. Conversely, positive effects conceivably associated with the use of a plug-flow filling strategy seemed to emerge towards the end of the operation, promoting the establishment of aerobic granules with high densities that caused a late rise in SVI in SBR2 concurrent with a continued decay in the settleability of the statically-fed SBR1. Even though some erratic COD and colour removal behaviours could be associated with the faulty nature of the plug flow, this configuration could prove helpful even in non-tubular bioreactors to secure stable aerobic granule structures.

AHL-based QS signalling as a reporter variable for sludge properties

AHL-based quorum sensing signalling proved an important feature of the aerobic granulation process, correlating positively with aerobic granulation. Like most other properties evaluated during this work, signal molecule levels proved higher in the lower shear environments of SBR1 during the initial stages of the AG life cycle. In the long run, however, detected AHL concentrations dropped significantly, which might suggest a lesser importance for QS mechanisms in AG maintenance. In aiming to explain the drivers behind this reduction, future studies should strive to analyze the importance of both QS and QQ in order to paint an integrated picture of quorum sensing regulation networks at all developmental AG stages and understand how the two processes balance each other. Combining a strategy to characterize the quorum quenching activity of aerobic granules with some method of QS molecule analysis and the community-level identification of signal producers and quenchers should provide relevant information.

References

[1] Lourenço, N. D., Franca, R. D. G., Moreira, M. A., Gil, F. N., Viegas, C. A., & Pinheiro, H. M. (2015). Comparing aerobic granular sludge and flocculent sequencing batch reactor technologies for textile wastewater treatment. Biochemical Engineering Journal, 104, 57-63.

[2] Van der Zee, F. P., & Villaverde, S. (2005). Combined anaerobic–aerobic treatment of azo dyes—a short review of bioreactor studies. Water research, 39(8), 1425-1440. Forgacs, E., Cserhati, T., & Oros, G. (2004). Removal of synthetic dyes from wastewaters: a review. Environment international, 30(7), 953-971.

[3] Sheng, Z., Van Nostrand, J. D., Zhou, J., & Liu, Y. (2018). Contradictory effects of silver nanoparticles on activated sludge wastewater treatment. Journal of hazardous materials, 341, 448-456.

[4] De Bruin, L. M. M., De Kreuk, M. K., Van Der Roest, H. F. R., Uijterlinde, C., & Van Loosdrecht, M. C. M. (2004). Aerobic granular sludge technology: an alternative to activated sludge?. Water Science and Technology, 49(11-12), 1-7.

[5] Singh, M., & Srivastava, R. K. (2011). Sequencing batch reactor technology for biological wastewater treatment: a review. Asia-Pacific Journal of Chemical Engineering, 6(1), 3-13.

[6] Dutta, A., & Sarkar, S. (2015). Sequencing batch reactor for wastewater treatment: recent advances. Current Pollution Reports, 1(3), 177-190.

[7] Muda, K., Aris, A., Salim, M. R., Ibrahim, Z., Yahya, A., van Loosdrecht, M. C., ... & Nawahwi, M. Z. (2010). Development of granular sludge for textile wastewater treatment. Water research, 44(15), 4341-4350.

[8] Franca, R. D., Vieira, A., Mata, A. M., Carvalho, G. S., Pinheiro, H. M., & Lourenço, N. D. (2015). Effect of an azo dye on the performance of an aerobic granular sludge sequencing batch reactor treating a simulated textile wastewater. Water research, 85, 327-336.

[9] Franca, R. D., Pinheiro, H. M., van Loosdrecht, M. C., & Lourenço, N. D. (2017b). Stability of aerobic granules during long-term bioreactor operation. Biotechnology advances.

[10] Jiang, B., & Liu, Y. (2012). Roles of ATP-dependent N-acylhomoserine lactones (AHLs) and extracellular polymeric substances (EPSs) in aerobic granulation. Chemosphere, 88(9), 1058-1064.

[11] Li, Y., Lv, J., Zhong, C., Hao, W., Wang, Y., & Zhu, J. (2014). Performance and role of N-acyl-homoserine lactone (AHL)-based quorum sensing (QS) in aerobic granules. Journal of Environmental Sciences, 26(8), 1615-1621.

[12] Lv, J., Wang, Y., Zhong, C., Li, Y., Hao, W., & Zhu, J. (2014). The effect of quorum sensing and extracellular proteins on the microbial attachment of aerobic granular activated sludge. Bioresource technology, 152, 53-58.

[13] Tan, C. H., Koh, K. S., Xie, C., Tay, M., Zhou, Y., Williams, R., ... & Kjelleberg, S. (2014). The role of quorum sensing signalling in EPS production and the assembly of a sludge community into aerobic granules. The ISME journal, 8(6), 1186.

[14] Liu, X., Sun, S., Ma, B., Zhang, C., Wan, C., & Lee, D. J. (2016). Understanding of aerobic granulation enhanced by starvation in the perspective of quorum sensing. Applied microbiology and biotechnology, 100(8), 3747-3755.

[15] Lee, D. J., Chen, Y. Y., Show, K. Y., Whiteley, C. G., & Tay, J. H. (2010). Advances in aerobic granule formation and granule stability in the course of storage and reactor operation. Biotechnology advances, 28(6), 919-934.

[16] De Kreuk, M. V., & Van Loosdrecht, M. C. M. (2004). Selection of slow growing organisms as a means for improving aerobic granular sludge stability. Water Science and Technology, 49(11-12), 9-17.

[17] Bassin, J. P. (2018). Aerobic granular sludge technology. In Advanced Biological Processes for Wastewater Treatment (pp. 75-142). Springer, Cham.

[18] Rocktäschel, T., Klarmann, C., Helmreich, B., Ochoa, J., Boisson, P., Sørensen, K. H., & Horn, H. (2013). Comparison of two different anaerobic feeding strategies to establish a stable aerobic granulated sludge bed. Water research, 47(17), 6423-6431.

[19] Franca, R. D. G., Ortigueira, J., Pinheiro, H. M., & Lourenço, N. D. (2017a). Effect of SBR feeding strategy and feed composition on the stability of aerobic granular sludge in the treatment of a simulated textile wastewater. Water Science and Technology, wst2017300.

[20] Zhang, C., Hu, Z., Li, P., & Gajaraj, S. (2016). Governing factors affecting the impacts of silver nanoparticles on wastewater treatment. Science of The Total Environment, 572, 852-873.

[21] Tang, J., Wu, Y., Esquivel-Elizondo, S., Sørensen, S. J., & Rittmann, B. E. (2018). How Microbial Aggregates Protect against Nanoparticle Toxicity. Trends in biotechnology.

[22] Gu, L., Li, Q., Quan, X., Cen, Y., & Jiang, X. (2014). Comparison of nanosilver removal by flocculent and granular sludge and short-and long-term inhibition impacts. Water research, 58, 62-70.

[23] Quan, X., Cen, Y., Lu, F., Gu, L., & Ma, J. (2015). Response of aerobic granular sludge to the long-term presence to nanosilver in sequencing batch reactors: reactor performance, sludge property, microbial activity and community. Science of the Total Environment, 506, 226-233.

[24] American Public Health Association (APHA), 1995. Standard Methods for the Examination of Water and Wastewater. In: Eaton, A.D., Clesceri, L.S., Greenberg, A.E. (Eds.), 19th ed. American Public Health Association, Washington, DC, USA.

[25] Tang, K., Zhang, Y., Yu, M., Shi, X., Coenye, T., Bossier, P., & Zhang, X. H. (2013). Evaluation of a new high-throughput method for identifying quorum quenching bacteria. Scientific reports, 3.

[26] Lemaire, R., Webb, R. I., & Yuan, Z. (2008b). Micro-scale observations of the structure of aerobic microbial granules used for the treatment of nutrient-rich industrial wastewater. The ISME Journal, 2(5), 528.

[27] Corsino, S. F., Capodici, M., Torregrossa, M., & Viviani, G. (2016). Fate of aerobic granular sludge in the long-term: the role of EPSs on the clogging of granular sludge porosity. Journal of environmental management, 183, 541-550.

[28] Toh, S., Tay, J., Moy, B., Ivanov, V., & Tay, S. (2003). Size-effect on the physical characteristics of the aerobic granule in a SBR. Applied Microbiology and Biotechnology, 60(6), 687-695.

[29] Feng, Q., Xiao, Y., Wang, X., Li, J., Wu, Y., Xue, Z., ... & Oleyiblo, J. O. (2016). The influences of shear stress on Extracellular Polymeric Substances of activated sludge. Desalination and Water Treatment, 57(34), 15835-15842.

[30] Bento, J. (2016). Interaction of silver nanoparticles with aerobic granular sludge in textile wastewater treatment bioreactors (MSc). Instituto Superior Técnico, Universidade de Lisboa.

[31] Rodrigues, A. (2017). Impact of engineered nanoparticles on the performance of aerobic granular sludge sequencing batch reactors treating textile wastewater (MSc). Instituto Superior Técnico, Universidade de Lisboa.

[32] Yang, Y., & Alvarez, P. J. (2015). Sublethal concentrations of silver nanoparticles stimulate biofilm development. Environmental Science & Technology Letters, 2(8), 221-226.

[33] Xiu, Z. M., Zhang, Q. B., Puppala, H. L., Colvin, V. L., & Alvarez, P. J. (2012). Negligible particle-specific antibacterial activity of silver nanoparticles. Nano letters, 12(8), 4271-4275.

[34] Clara, M., Kreuzinger, N., Strenn, B., Gans, O., & Kroiss, H. (2005). The solids retention time—a suitable design parameter to evaluate the capacity of wastewater treatment plants to remove micropollutants. Water research, 39(1), 97-106.

[35] Li, Y. C., & Zhu, J. R. (2014). Role of N-acyl homoserine lactone (AHL)-based quorum sensing (QS) in aerobic sludge granulation. Applied microbiology and biotechnology, 98(17), 7623-7632.

[36] Chen, H., Li, A., Cui, D., Wang, Q., Wu, D., Cui, C., & Ma, F. (2018). N-Acyl-homoserine lactones and autoinducer-2-mediated quorum sensing during wastewater treatment. Applied microbiology and biotechnology, 102(3), 1119-1130.

[37] Song, X. N., Cheng, Y. Y., Li, W. W., Li, B. B., Sheng, G. P., Fang, C. Y., ... & Yu, H. Q. (2014). Quorum quenching is responsible for the underestimated quorum sensing effects in biological wastewater treatment reactors. Bioresource technology, 171, 472-476.

[38] Tan, C. H., Koh, K. S., Xie, C., Zhang, J., Tan, X. H., Lee, G. P., ... & Kjelleberg, S. (2015). Community quorum sensing signalling and quenching: microbial granular biofilm assembly. npj Biofilms and Microbiomes, 1, 15006.

[39] Li, Y. S., Cao, J. S., Li, B. B., Li, W. W., Fang, F., Tong, Z. H., & Yu, H. Q. (2016). Outcompeting presence of Acyl-Homoserine-Lactone (AHL)-quenching bacteria over AHL-producing bacteria in aerobic granules. Environmental Science & Technology Letters, 3(1), 36-40.